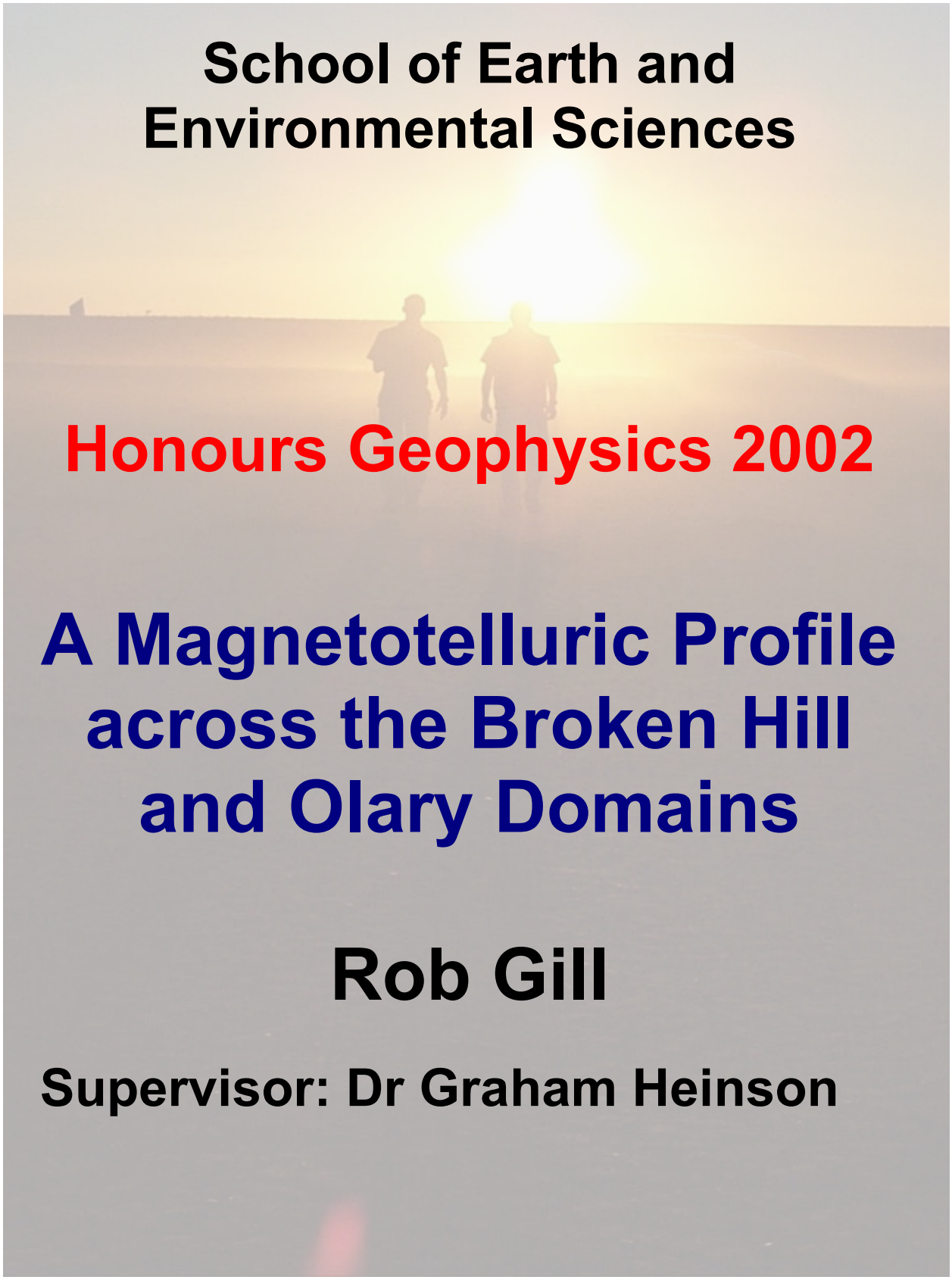

THE UNIVERSITY OF ADELAIDE
AUSTRALIA

SUB CRUCE LUMEN

School of Earth and Environmental Sciences

Honours Geophysics 2002

A Magnetotelluric Profile across the Broken Hill and Olary Domains

Rob Gill

Supervisor: Dr Graham Heinson

Table of Contents

A Magnetotelluric Profile across the Broken Hill and Olary Domains

R.M. GILL

School of Earth and Environmental Sciences, University of Adelaide

Adelaide SA 5005 Australia

Robert.Gill1@defence.gov.au

Seventeen magnetotelluric survey sites were occupied across the Olary and Broken Hill Domains in the Curnamona Province, Australia. Two dimensional modelling along the magnetotelluric profile identifies the Broken Hill Domain as a zone of high electrical resistivity to a depth of 15km. Gravity modelling along a coincident profile has also shown the Broken Hill Domain to be significantly more dense than its surrounds. Seismic data have provided evidence of numerous faults and shear zones within the Pre-cambrian Broken Hill Domain basement, and is indicative of compression during the Delamarian Orogeny. It is proposed that the majority of crustal fluids were removed from these rocks by granulite facies metamorphism and tectonic compression. The boundary of the Olary Domain appears to be delineated by the Mundi Mundi Fault with an order of magnitude increase in resistivity on the Broken Hill side. The location of the Flinders Conductivity Anomaly was also observed and a number of conducting mechanisms considered, including crustal fluids and graphite films.

Key words: Curnamona Province, Olary Domain, Broken Hill Domain, Magnetotellurics, Geomagnetic Depth Sounding, Electrical Resistivity Modelling.

INTRODUCTION

The Curnamona Province extends across eastern South Australia and western New South Wales, is sub-circular in shape and comprises outcropping and relatively shallowly buried Proterozoic basement rocks (Robertson et al. 1998) (Figure 1). Aeromagnetic data have delineated the province, and shown it to be fringed by younger mobile belts (Robertson et al. 1998). The term Curnamona Cratonic Nucleus was first applied by Thomson (1970) for the central part of the province, which he described as being cratonic in character during the Delamarian Orogeny. Subsequent drilling indicated that this central region had been cratonic even earlier than this (Robertson et al. 1998). The Adelaidean and Cambrian cover sequences are undeformed, and the underlying suite of Mesoproterozoic sedimentary and volcanic rocks do not show signs of substantial metamorphism and tectonism. The term was abbreviated to Curnamona Craton by Flint (1993), but by this stage aeromagnetic data sets suggested the tectonic integrity of the entire province. Hence the term was used to cover the entire aeromagnetically defined zone, including outcropping pre-Adelaidean basement rocks, and the non-genetic term 'Curnamona Province' was applied (Robertson et al. 1998). The known units of the Curnamona Province can be divided into two distinct groups; the oldest is a late Palaeoproterozoic metasedimentary and partially metavolcanic succession, the Willyama Supergroup; the second (and youngest) includes intrusives that experienced intensive tectonism and metamorphism during the Olarian Orogeny. (Robertson et al. 1998)

Within the Curnamona Province, two distinct regions have been identified; the Olary and Broken Hill Domains. This sub-division was first made by Thomson (1976). From initial analysis, Thomson chose the SA-NSW border as an arbitrary domain boundary. Subsequent interpretations have proposed a domain boundary based upon an elongate northeast trending magnetic low region west of Cockburn on the South Australia/New South Wales border (Isles 1983; Mills 1986; Stevens 1986; Ashley et al. 1997). This magnetic feature has been identified by geological mapping as a major shear, with Sundown and Paragon Group pelitic schists and kyanite bearing Strathearn Group rocks in the west brought into juxtaposition with demagnetised Wiperaminga Subgroup and Thackaringa Group quartzo-feldspathic leucogneisses in the east. These geological criteria can transgress the shear zone, and therefore on geological grounds its significance as a domain boundary has little validity (Crooks 2001).

There are varied proposed settings for the deposition of the Willyama Supergroup, including shallow marine shelf and marine platform environments and intercratonic basins (Thomson 1976). This interpretation was based upon the extensive distribution of a thick sequence of thinly bedded sediments, the minimal occurrence of sub-aerial volcanics and the lack of coarse clastics (Rutland 1976; Willis et al. 1983). From palaeogeographic studies, Stanton (1976) inferred a horst and graben structure with shelves, basins and volcanic rises. The most accepted tectonic setting for the deposition of the Willyama is a volcanically active, failed intracontinental rift setting with initial intercalated terrestrial, lacustrine/sabhka and marine sequences succeeded by deeper marine/lacustrine sequences (Willis et al. 1983; Ashley et al. 1996). Interpretations of the Olary Domain succession suggest it having been deposited in a continental

lacustrine environment, deepening upwards into a marine environment (Cooke & Ashley 1992). In comparison, the Broken Hill Domain has been suggested to represent a deepening marine succession incorporating basic and felsic volcanics deposited in a developing rift (Wills et al. 1983, Stevens et al. 1988; Stevens 1995). Robertson et al. (1998) therefore suggest that the Olary Domain may have been marginal to the rift.

Both the Olary and Broken Hill Domains show similar complex depositional, tectonic, metamorphic and intrusive history, and provisional lithostratigraphic correlations have been made (Campana & King 1958; Flint & Flint 1975; Willis et al. 1983; Clarke et al. 1986; Stevens et al. 1990; Cooke & Ashley 1992; Flint & Parker 1993; Laing 1996). However the higher proportion of shallow water sediments, fewer volcanics, extensive metasomatism (predominantly albitisation) and the prevalence of syntectonic to late-tectonic granitoid intrusions within the Olary Domain indicate significant differences (Robertson et al. 1998). Clarke et al. (1986) proposed a sequence for the Olary Domain which was broadly correlated to the Broken Hill Domain, and recent work by Conor (2000) has provided a formal lithostratigraphic scheme for major subdivisions of the Olary Domain, and comparison of these with those of the Broken Hill Domain.

The Mundi Mundi Fault (MMF) trends north-north-easterly, and separates the western margin of the Barrier Ranges from the alluvial Mundi Mundi Plain (Gibson 1997). The location of the fault is readily identifiable due to the marked change in elevation and topography; from the flat expanse of the Mundi Mundi Plain to the rugged hills of the Barrier Ranges, as shown in Figure 2. For much of its length the fault is concealed by alluvium, however Geoscience Australia seismic reflection data (Gibson et al. 1998)

indicates that it is a major crustal structure dipping at approximately 30° to the East. It has been suggested (Gibson et al. 1998; Clarke et al. 1987) that this fault in fact marks the contact between the Olary and Broken Hill Domains.

A magnetotelluric (MT) traverse was conducted approximately perpendicular to the Mundi Mundi fault, stretching from Kalkaroo to the north-west of Broken Hill to approximately 40 km to the south-east of Broken Hill along the road to Menindee. The MT traverse was conducted in a similar location to that of the seismic line (Gibson et al. 1998), however due to logistical issues was not run directly over it, as shown in Figure 3. This study was conducted predominantly to further investigate the contact between the Olary and Broken Hill Domains and the significance of the Mundi Mundi Fault. Additional to this primary aim, the logistics of conducting land MT surveys was investigated, with the aim of providing suggestions for improvement of equipment and deployment. Correlation of MT data with previous studies in the area, including seismic and airborne and ground geophysical surveying, was also carried out.

Little is known of the electrical resistivity properties of the crust in the Curnamona Province. In 1982 an MT survey was conducted in the Broken Hill region by Cull (Cull 1985; Gray & Cull 1990). The location of these sites closely follows those of the current work, with the eastern most station of the 1982 survey being located in close proximity to station 9. From here, the 1982 survey follows the same path, along the Broken Hill to Menindee road, however where the current study terminates around 30km south-east of Broken Hill, the 1982 line extends past Menindee to Ivanhoe (Figure 3). A further study in the area in 1984 (Gray & Cull 1990) incorporated two

MT lines, one running south from Broken Hill, and the other heading east, with the initial site approximately 20 km to the east of Broken Hill. Data acquired from these surveys provided more detailed information regarding the transition from the Broken Hill Domain to the sediments of the Murray-Darling Basin. Marked anisotropy was noted in their data, with different estimates of resistivity arising from variations in direction of measurement. This regional anisotropy was attributed (Cull 1985; Gray & Cull 1990) to lateral discontinuities in sub-crustal structure, suggesting major crustal lineaments east of Broken Hill. These may have been generated by progressive migration from an accretionary boundary associated with evolution of the Proterozoic terrains (Katz 1976). Models were also put forward based upon rifting followed by total subduction.

A number of regional electrical conductivity studies have been conducted over the Australian continent (Chamalaun & Barton 1993; Wang et al. 1997; Wang & Chamalaun 1995; Chamalaun and Barton 1990; Chamalaun 1985; Paul 1994). These have been broad scale in nature, however have covered the area of interest in this study. These studies have typically involved the deployment of a number of Geomagnetic Depth Sounding (GDS) stations with broad spacing. From such work, the conductivity structure of large areas of the Australian continent has been mapped, predominantly with the use of Parkinson Induction arrows (Parkinson 1962). These earlier investigations provide a framework within which this survey can be viewed, particularly with regard to previously identified and delineated conductivity anomalies.

MAGNETOTELLURICS & GEOMAGNETIC DEPTH SOUNDING

The magnetotelluric method utilises natural sources of time-varying magnetic fields, including those caused by magnetic storms and solar flare activity. These fields penetrate into the earth, and as a result induce electric and secondary magnetic fields (Vozoff 1972). We can measure the total magnetic and electric fields at the earth's surface. All three components of the magnetic (magneto) field **H** are measured, and these are notated as $\mathbf{H_x}$, $\mathbf{H_y}$ and $\mathbf{H_z}$, where x and y denote orthogonal horizontal components, and z vertical. Figure 4 shows an example of time series magnetic data from the current study. For the electric (or telluric) field **E**, the two orthogonal horizontal components $\mathbf{E_x}$ and $\mathbf{E_y}$ are measured. An example of electrical time series data from the current study is shown in Figure 5. Measurements of these quantities are made in the time domain, and then transformed to the frequency domain.

We can define an MT impedance tensor: $\begin{pmatrix} Z_{xx} & Z_{xy} \\ Z_{yx} & Z_{yy} \end{pmatrix} \begin{pmatrix} H_x \\ H_y \end{pmatrix} = \begin{pmatrix} E_x \\ E_y \end{pmatrix}$

In this equation, H are inducing fields, E are induced fields and the tensor elements Z_{ij} represent the Earths electrical impedance. The apparent resistivity, ρ_a, of the conductor can be determined from the equation: $\rho_a = \frac{2x10^{-7}}{\mathrm{T}} \left| \frac{E_x}{B_y} \right| = \frac{2x10^{-7}}{T} \left| Z_{xy} \right|^2$

Phase is defined by $\phi_{xy} = \tan^{-1} (Z_{xy})$.

The bandwidth of frequencies used in MT is about 10^{-4} to 10^{4} Hz (Periods of 10^{4} and 10^{-4} s). In an earth with bulk resistivity of 100 Ωm, this corresponds to a range of skin depths from 50 m-500 km. With an increase in depth, and hence reduction in frequency, resolution is decreased. Figure 6 shows an example of MT data from station 15, namely apparent resistivity and phase against period.

Induction Arrows

Induction arrows describe the linear relationship between the components of the vertical and horizontal magnetic variation fields. When displayed on a map they facilitate the identification of the orientation and qualitative intensity of crustal conductivity anomalies (Parkinson 1962; Everett & Hyndman 1967; Schmucker 1970).

A varying external magnetic field will induce electric currents within the earth. Where the electrical conductivity structure of the earth is not homogeneous, a vertical magnetic field, Z, will be generated by the induced currents, and its fluctuation is correlated with the horizontal field.

An induction transfer function can be use to describe this relationship:

$$Z_\omega = A_\omega X_\omega + B_\omega Y_\omega$$

X and Y are the north and east components of the external horizontal field, A and B are the transfer function coefficients that describe the correlation between the vertical and horizontal fields at a particular location, and ω is the frequency. All of the quantities involved are complex, and the Fourier transforms are used to compute the transfer functions for a variety of frequencies. As the depth-penetration of electromagnetic

waves is inversely proportional to the square root of the frequency, information regarding the depth of induced currents can be deduced from the transfer function coefficients, A and B, which are frequency dependent. The depth of penetration is governed by the skin depth equation, $\delta = 500\sqrt{\rho T}$.

An expression for X in terms of real (X_r) and imaginary (X_q) can be used;

$$X = X_r + X_q$$

And also for Y, Z, A and B such that;

$$Z_r = A_r X_r + A_q X_q + B_r Y_r + B_q Y_q$$

$$Z_q = A_r X_q + A_q X_r + B_r Y_q + B_q Y_r$$

The induction arrow is derived from the quantities A and B, and for Parkinson arrows (Parkinson 1962), points toward the induced current concentration in the nearest conductor. Its length, R_ω, and azimuth, θ, are found from:

$\theta = \tan^{-1}(-B_\omega/-A_\omega)$, [$\theta$ Clockwise positive measure from north] ; $R_\omega = \sqrt{(A_\omega^2 + B_\omega^2)}$

The time dependence factor used for the spectral analysis of a time series of geomagnetic data is either $e^{i\omega t}$ or $e^{-i\omega t}$. Here ω represents the angular frequency in radians and t the time. When $e^{i\omega t}$ time dependence is used, as is the case in this study, the Parkinson convention (Parkinson 1962) dictates that the real and quadrature arrows be reversed in order to point towards near-surface in-homogeneity (Lilley & Arora 1982).

DATA COLLECTION

Four Flinders University High Frequency MT sensors were used for this study, and involved modifications to convert the sensors from marine to land instruments. This work was conducted by technical staff at Flinders University, and involved replacing the D-cell batteries with connections for two 12 V truck batteries, the installation of sockets for the electrode arrays and mounting within water-proof protective cases. Each instrument comprised a fluxgate magnetometer and an electrode array consisting of north-south and east-west electrode pairs for which ceramic pot electrodes were used with a $CuSO_4$ electrolyte. An onboard computer program logged the inputs at a sampling frequency of 20 Hz, and stored the data blocks on a flash card that could later be removed and connected to a PC for download. The program also permitted the logging process to commence at a particular time and date, and hence enabled the one survey crew to deploy multiple sites, all of which could be set to commence logging at the same time. In this manner, stations could be used as remote reference for each other, reducing noise and improving data quality (Gamble et al. 1979).

Seventeen deployment sites were chosen with an approximate spacing of 10 km between each, and their locations are shown in Table 1 and Figure 7. At each site one set of MT equipment was buried to a depth of approximately 10 cm, and the electrodes deployed such that the north and east components were on 100 m cables, and the south and west components on 20 m cables. This resulted in the electrodes of each pair (north-south and east-west) being separated by 120 m (Figure 8). Initial deployments lasted for approximately two days with a sampling interval of 20 Hz, however this was

ultimately reduced to approximately one day. It was found after the initial deployments that the electrodes became unstable, either due to the evaporation/seepage of the electrolyte or removal of the lids by native animals. Field analysis of data suggested that approximately one day of data was sufficient.

After the required deployment time had been reached, the instruments were recovered and the data transferred to a PC. Initial processing was conducted in the field, and involved visually inspecting the magnetic and electric field data to ascertain whether each deployment had been successful. Examples of magnetic and electric time series data are shown in Figures 4 & 5. In the electric field (Figure 5), field readings change abruptly just before 33hours ($12x10^4$ s). After this point, the readings vary erratically, and this signifies either the loss of the entire $CuSO_4$ electrolyte or the removal of the electrode lid.

At this stage in the processing another difficulty with the electric field readings was identified. Whilst there are likely to be times when both components of the electric field are correlated, at some sites both channels appeared very similar. It is believed that internal leakage in the amplifier electronics occurred due to high impedance contacts at the electrodes and/or capacitance effects with the long wires. The impact on the data acquired is that only the magnetic field data can be relied upon. The result of this is that when running the 2D inversions later in the processing sequence, only the vertical (H_z) transfer function component was selected for inversion. The TE and TM mode resistivity and phase data were therefore not used at this stage.

The raw data, initially in binary format, were converted to ASCII at one-second averages. Both MT and GDS transfer functions were determined using the RRRMT program written by Dr Alan Chave (Chave et al. 1987; Chave & Thompson 1989). The GDS responses from site 10 can be seen in Figure 9. The minimal size of the majority of the error bars indicate high data quality, with the exception of the higher frequencies (short period) where the data are affected by noise. Data were then imported into the WinGLink program, an application created by GEOSYSTEM (WinGLink® User's Guide, Release 1.55 2002), and then modelled using 2D inversion software (Rodi & Mackie 2001).

OBSERVATIONS & RESULTS

Two-Dimensional Modelling

The 2D inversion process within Winglink involves a smooth model inversion routine developed by R Mackie (Rodi & Mackie 2001). The routine finds regularized solutions (Tikhonov Regularization) to the 2D inverse problem for MT data using the method of non-linear conjugate gradients. The forward model simulations are computed using finite-difference equations generated by networks analogs to Maxwell's equations. The program inverts for a user-defined 2D mesh of resistivity blocks, extending laterally and downwards beyond the central detailed zone.

A profile along the survey line was chosen as shown in Figure 3, and all MT survey sites selected, enabling data from each station to be used in the inversion process. The

vertical magnetic transfer function data (H_z) was selected to be input into the inversion algorithm. The H_z component was modelled, with a bandwidth of 0.1-0.00001Hz (period of 10-10000s). A range of 2D smooth inversions over the MT line (with elevation included) were run. In each case, 200 iterations were carried out, and a number of different floor-errors selected. Error estimates on MT and GDS transfer functions are calculated by RRRMT by the Jacknife method (Chave & Thomson 1989; Thomson & Chave 1989) but in modelling it is useful to pre-set a minimum error (or error floor). If RRRMT derived errors are smaller, the program then fixes the error to the selected error-floor. The optimum absolute floor error for this data was 0.045, and this resulted in an RMS error of 1.0 (Figure 10).

Immediately apparent in Figure 10 is a marked conductivity contrast between the western and eastern parts of the section, in the order of 500Ωm. A highly resistive region can be observed in the vicinity of stations 09-13. The surface location of this transition is slightly to the east of station 9. This is coincident with the location of the Mundi Mundi Fault, and the corresponding abrupt change in topography between the Mundi Mundi alluvial plain to the west, and the Barrier Ranges to the east. Not only is the fault evident, but its listric nature is also apparent, with a marked curvature in the fault contact on the 2D section. Although the resolution of the modelling is approximately equal to the depth of investigation, it is evident that the principal dip of the fault is imaged. The region of high resistivity to the east of the fault correlates with the location of the Broken Hill block, a region of more resistive Pre-cambrian basement.

From both the 1982 (Cull 1985) and 1984 (Gray & Cull 1990) MT surveys, a highly resistive region (1000 Ωm) incorporating Broken Hill was identified, contacting with much more conductive sediments of the Murray-Darling Basin to the East. Recent sediments exhibited resistivities ranging from 1-10 Ωm, whilst those of the Devonian ranged from 10-100 Ωm. The 2D section in Figure 10 supports this, and comparison of resistivity values with those of the two earlier surveys provide similar resistivities for the Broken Hill Domain, in the order of 1000 Ωm. These values are reasonably consistent with those obtained by Constable (1985) from DC soundings in the Broken Hill region.

Comparison with Seismic Data

Jones (1987) discussed the advantages of conducting MT studies in conjunction with seismic surveys. He indicated that the high lateral resolution of MT data can be very useful in distinguishing sub-vertical faults, which are not often as readily identifiable from seismic reflection sections. The increased lateral resolution of MT methods is due to the fact that the essential parameter for MT responses, resistivity, can vary over many orders of magnitude (10^{-1} – 10^{6} Ωm), whilst seismic parameters may vary by less than one order of magnitude. MT is particularly helpful when imaging faults which juxtapose blocks of differing conductivity, as is seen to be the case with the Mundi Mundi Fault. The seismic method experiences difficulties when applied to basement terrains, as such targets often include steep structure, including folds and faults, which are not always readily imaged (Gibson et al. 1998).

The AGSO seismic survey (Gibson et al. 1998) was able to identify a number of crustal structures. A significant number of south-east dipping reflectors were observed, corresponding to a series of thrust faults and shear zones. This evidence of strong compression was attributed to tectonism of the Delamarian Orogeny or earlier. The AGSO seismic line has been able to identify the location and orientation of the fault, however the 2D MT inversion section has highlighted the contrasting properties of the rocks either side of the fault. The angle observed from the inversion section is approximately 25°, and given the low vertical resolution of the MT data this corresponds well with the angle, approximately 30°, calculated from the AGSO seismic survey (Figure 11) (Gibson et al. 1998). It is therefore apparent that the utilisation of MT surveying in conjunction with seismic surveying provides a more detailed picture of crustal geology, and compensates for the difficulties when using seismic surveying for such investigations.

Gravity Modelling

Gravity data have been collected and collated by Geoscience Australia (Milligan et al. 2000). From this data set a section of Bouguer anomaly gravity data was plotted, along the same profile as that used for MT, and initial gravity modelling conducted, as shown in Figure 12. The most striking aspect of the gravity data is the increased Bouguer gravity over the Broken Hill Domain, with a peak anomaly of about 15 mGals. Over the Olary Domain the gravity anomalies are negative, at around –10 mGals. Upon early inspection it was apparent that the variations in observed gravity are roughly coincident with regions of differing conductivity. Bodies were superimposed over these

conductive and resistive regions, and relative densities applied as follows: A mid-lower crust of 3.1 g/cm^3, a resistive Pre-cambrian Broken Hill Domain of 3.31g/cm^3, low density sediments of the Olary Domain (2.0 g/cm^3 and 2.8 g/cm^3) and a region associated with the FCA of 2.4 g/cm^3. Density values and sediment structure were assigned using the AGSO Curnamona Geophysical Atlas as a guide (Milligan et al. 2000). The resultant model response was reasonably close to the observed data, however no rigorous fitting was undertaken. The density distribution of these regions is obviously far more complex than shown in the modelling, however the broad scale nature of the gravity profile was of interest rather than a higher resolution model.

Although, as mentioned, the assigned values are by no means precise or truly representative, the modelling does however indicate that there is perhaps some broad scale correlation between conductivity and density in the study region, and further, more exhaustive work may lead to interesting results. Highly compacted, and therefore dense rocks may experience high electrical resistivity as a result of this compaction. The compaction process leading to higher density will reduce pore space, and hence the volume of fluids contained within the rocks will be reduced. This reduction in available pore space will significantly reduce electrical conductivity, since even small amounts of crustal fluids will give rise to significant electrical conductivity compared with dry rocks. Other conducting mechanisms, such as graphite films and partial melts, may be present in the absence of fluids, and therefore provide a means by which other, similarly dense regions may exhibit higher conductivity.

Induction Arrows

Real Parkinson induction arrows from the MT profile for 0.0001 Hz (T~166 mins) are shown in Figure 7. Although little could be deduced from these arrows alone, the fact that they are reasonably consistent, and variations in orientation are smooth and gradual, further adds to our confidence in the data acquired. Data of poor quality are likely to lead to erratic magnitudes and orientations of the induction arrows. Also evident from the inversion section is a region of high conductivity near the western edge of the survey. This corresponds very well to the interpreted location of the Flinders Conductivity Anomaly (FCA). The FCA was first identified by Gough et al. (1974) during a 2D magnetometer array study in South Australia. Further investigations were made by Chamalaun (1985), who proposed a northward extension of the earlier interpretation, to the east of Lake Frome.

Paul (1994) conducted a significantly more detailed study of the FCA, and his interpretation of its location is shown below in Figure 13. He suggested that the depth to the top of the conductor was between 10 and 20 km, that it is funnel shape in section and has a stem extending into the mantle to a depth of around 35 km. The 2D modelling from the current study does not extend further westward, and hence the FCA can be identified but not accurately constrained, as it extends outside the scope of the profile. The apparent depth to the top of the major part of the conductor from this section is approximately 10 km, and therefore consistent with the observations of Paul (1994).

To delineate the FCA on a regional scale in the Olary Domain, induction arrows plotted from the current experiment have been added to the data from Paul (1994) (provided by Geoscience Australia) as seen in Figure 14. Arrows were plotted for a sub-section of the original arrows of Paul (1994), and allowed a more accurate, higher resolution interpretation of the path of the FCA in the vicinity of Kalkaroo (Figure 14). Interpretation of individual arrows can be complicated due to localised variations in geology (Greenhouse & Bailey 1981), and hence some arrows do not point directly toward the inferred location of the FCA. On a broader scale however, the real arrows point towards a region of higher electrical conductivity in the crust over many hundreds of kilometres. Given the spacing of the stations, it is not clear if the crustal conductors are continuous, or in discrete regions.

Paul (1994) proposed that the FCA was possibly caused by a ductile shear zone between two cratonic plates which were rifted apart and later compressed together, or a ductile shear zone which accommodated relative motions between two intercratonic plates. Woods & Lilley (1980) suggested that the FCA was possibly linked with the Southwest Queensland Anomaly, however Paul (1994) proposed that there is in fact a break between the two.

Instrumentation

One desired outcome of this surveying was to investigate the logistical aspects of using the modified Flinders University MT equipment for terrestrial surveying. Overall, this system was found to be very user friendly. The procedure for establishing a survey site

and initialising the sensor was relatively simple to complete, and the computer logging program in particular was very user friendly. Deployment of the electrodes and associated cabling was the most time consuming step, however due to the sparsity of vegetation in the field area, orientation was easy, as in almost all situations the sensor was clearing visible at each electrode site. This facilitated the accurate deployment of the electrode arrays.

After deployment of the first two survey sites, two issues concerning the electrode arrays were identified. The first was the dislodgment of electrode stoppers or breaking of wires, resulting in a loss of signal from the relevant electrode pair. It is believed that native and pastoral animals disturbed the electrodes in such cases. It was proposed that native animals such as kangaroos may have tripped on cabling held slightly above ground level by vegetation, and that sheep had, in places, chewed through the wiring. These difficulties were significantly reduced by ensuring that all cables were run flat along the ground, and where possible weighted or covered.

The other significant factor affecting electrode performance was the dryness of the topsoil. Even though the survey was conducted in winter, the soil in the study area was very dry. It is believed that this caused the rapid seepage of electrolyte through the porous walls of the electrodes and into the parched soil. A possible solution to this problem is the replenishment of electrolyte during deployments, however this was not carried out during the field work. If this were to be attempted during future surveys, care would need to be taken to ensure minimal disruption to recording.

Initially both the sensor and its batteries were buried, however as the soil in most cases was difficult to excavate, it was decided that the battery box would simply be placed on the surface. The weight of the batteries themselves ensured they were not dislodged by significant winds. This did however mean that the survey site was readily identifiable from a distance, and whilst not a major concern in this study, in populated areas this could invite vandalism or theft of the survey equipment. When configured for marine surveying, the sensors were powered by disposable power packs of 1.5 V D cell batteries. For land surveying these were replaced by two 12 V truck batteries, which could be re-charged and used again. For this study, adequate transport was available to transport the large number of truck batteries required. For surveys with minimal logistical support however, the original power packs may be more convenient.

After the survey team became experienced in preparing the MT sites, deployment time was reduced to around 15 mins. This enabled the complete turn-around of four sites in a day, including instrument recovery from existing sites and subsequent occupation of new sites and commencement of logging. Toward the end of the survey one team member remained to deploy and recover the remaining sites, and was able to establish a site in around 30 mins. This relative ease of deployment/recovery enabled expedient collection of data over a large survey area.

DISCUSSION

As can be observed in the 2D modelling, the Broken Hill Domain has been shown to be highly resistive in comparison to surrounding regions, including the Olary Domain. In

addition to it being highly resistive (~1000 Ωm), it is also shown to be associated with a large gravity high, and hence is also more dense (~2.8-3.3 g/cm^3) than its surrounds. Seismic data (Gibson et al. 1998) has shown a number of easterly dipping faults and shear zones within the Broken Hill Domain. These structures suggest thrusting and exhumation resulting from significant compression during the Delamarian Orogeny. There is however evidence of earlier extensional structures. A proposed mechanism for this paradox is that the rocks of the Broken Hill Domain were exceptionally dry following granulite facies metamorphism. The earlier rift geometry would therefore have been 'locked' in place, with the absence of fluids inhibiting movement of the existing structures. This hypothesis also explains the high (~1000 Ωm) resistivities of the Pre-cambrian Broken Hill Domain. The minimal presence of fluids following metamorphism, and the expulsion of any that remained during the subsequent compression appears to have drastically reduced the ability of these rocks to conduct electricity. The surrounding sediments of both the Mundi Mundi Plain and the Murray Darling Basin are much more conductive (1-100 Ωm) due to pore fluids, and of lower density (~2.6 g/cm^3). These sediments, with their higher porosity, would readily hold the volume of fluid required to facilitate their higher conductivity. This increased pore space also reduces their density, as opposed to highly compacted basement rocks.

Also evident from the 2D inversion is the presence of highly conductive regions in the mid to lower crust, including the FCA. Gray and Cull (1990) also observed regions of deep-seated conductive material from their MT surveying. Values assigned from their 2D modelling indicated a resistivity of around 100Ωm beneath the Pre-cambrian basement. This value is similar to that arising from 2D inversions generated during the

current work, in which the resistive Broken Hill Domain terminates at a depth of around 15 km. Earth materials conduct electricity predominantly by the flow of ions in fluids, and the flow of electrons in solids. Dry silicate rocks for example are highly resistive, so a region of enhanced electrical conductivity represents an interconnected network of a fluid and/or mineral conducting phase (Jones & Ferguson 2001). The causes of high crustal conductivity can be broadly divided into four mechanisms: fluids, carbon films, conducting minerals and partial melts.

Attributing high conductivity of the crust to saline fluids is an attractive proposition, as even small volumes of such fluids greatly improve electrical conductivity. The feasibility of fluids in the crust has been questioned however. Whilst deep crustal fluids may well exist in active regions (where fluid recharge may be possible), it is generally understood that any fluids at such depths would migrate toward the surface (Bailey 1990; Bailey 1994). In stable regions, crustal brines with low density would tend to percolate toward the surface, leaving the hot, ductile crust in geologically short periods (Simpson & Warner 1998). If they are to remain within the crust, some trapping mechanism must be present. Gough (1986) suggested that saline fluids permeate the whole crust, and are under compressive stress in the upper crust and hence in separated cavities, whilst in the lower crust the fluids form interconnected films on the crystal surfaces. The latter case would then facilitate high conductivity.

Marquis & Hyndman (1992) explored pore geometry as a means of retaining fluids at depth, and hence accounting for high conductivities in the crust. For this situation to arise, low vertical permeability is needed to retain fluids at depth, whilst high horizontal

permeability is required to maintain high horizontal conductivity. A model accounting for such characteristics involves deformation of pores by small deviatoric stresses. It has been observed that very small compressive stresses (200 Pa) can pinch off vertical pores that would otherwise be interconnected, whilst retaining horizontal pore interconnection. In this way, fluids are inhibited from vertical migration (preventing escape) whilst still being connected horizontally, and hence enabling high conductivity in this orientation. Kusznir & Park (1986) investigated the presence of such stresses in the crust.

Merzer & Klemperer (1992) suggested that the crust may be comprised of permeable, conductive lamellae. This could enable the lithological trapping of saline water in these lamellae, within an impermeable, non-conductive matrix. These lamellae are thought to be un-connected, and hence conductivity may be due to the mutual overlapping of conductive regions. If these regions were connected the conductivity would be significantly increased, yet it is expected that if this were the case, the fluids would leak from the crust. Another mechanism described by Marquis & Hyndman (1992) involves the presence of crustal shear zones. As horizontal motion (eg. extension) occurs, the crust may be progressively deformed in layers as the temperature of the brittle-ductile transition progresses downwards. The differential slip between layers produces deep crustal shear zones in which high-pressure fluids may be trapped. As a result of this, a series of inter-bedded horizontal layers of fluid with good horizontal interconnection may be present, but with vertical migration restricted.

A more recent explanation for the observed high conductivity of the crust is the presence of carbon films on grain boundaries. Fluid inclusion studies of the Laramic Anorthosite Complex (1.4 Ga) indicate that the rocks crystallised at pressures of 3 kbar and temperatures of 950-1030° in the presence of graphite and almost pure CO_2-CO vapour phase (Frost et al. 1989). Graphite films with thickness of ≈ 1,000 Å were observed. Frost et al. (1989) suggested that the presence of these films may facilitate the high conductivity of the crust. This phenomenon appears to be dependent on depth. At depths where the temperatures exceed rock crystallisation temperatures, CO_2 is no longer a candidate as it is an insulating liquid and a non-polar gas and hence has little or no effect on electrical conductivity. Conversely, at shallow depths crystallising rocks may not reach graphite saturation.

Carbon films on grain boundaries have also been suggested (Jödicke 1985) to account for the low resistivity of black shales (2-3 Ωm). Duba et al. (1988) studied Carboniferous samples of black shales which had been extracted from a 5425 m deep borehole in northern Germany. The organic component of these rocks was found to consist of ≈ 95 % carbon. At high frequencies, electrical impedance was shown to have a high dependence on bedding direction. At frequencies relevant for deep geophysical studies (lower than 17 Hz in their experiments) the data were almost frequency-independent. Their studies showed that the conduction mechanism was controlled by an interconnected phase. This seemed to confirm Jödicke's suggestion that low resistivity was caused by a thin film of carbon on the grain boundaries.

Frost et al. (1989) investigated the occurrence of graphite in rocks, and the implications of this for the high electrical conductivity observed in the crust. They proposed two causes of this increased conductivity. The first is that graphite stability is enhanced by pressure. Therefore, a mafic rock crystallising in a shallow environment may not reach graphite saturation even upon cooling. One cooling at greater depths is more likely to develop grain-boundary graphite. The second cause suggested is loss of conductivity with decompression. Grain-boundary graphite will act as a strong conductor only if the film is continuous. During decompression it is expected that the development of fractures along the grain boundaries would remove the continuity of the graphite film, and hence the conductivity of the rock.

It has been suggested (Olhoeft 1981) that conducting minerals (eg. sulphides) may contribute to the enhanced conductivity of certain parts of the crust. MT studies in northern Montana and south-eastern British Columbia have shown conducting zones that have been attributed to sulphides in belt rocks. Drilling in the area appears to have confirmed this interpretation.

Laboratory studies have shown that partial melts increase the conductivity of rocks by several orders of magnitude. (Waff 1974; Sato & Ida 1984). It is believed that partial melts may give rise to the high conductivity of the crust in Northern Tibet. (Wei et al. 2001) A conductance of ~20,000 S is observed in a conductor located at a depth of around 40 km. In this region, satellite magnetic data, high heat flow and young granites all indicate high crustal temperatures. It is suggested that radiogenic heating has given rise to the elevated temperatures needed to initiate partial melting during crustal

thickening. The Olary Domain has a much greater occurrence of granites and granitoids than does the Broken Hill Domain, and hence current partial melts may well be a contributing factor to the conductive regions within it.

Also of interest is the continuing conundrum of the location of the boundary between the Olary and Broken Hill domains. In previous work the Mundi Mundi Fault has been put forward as the contact between the two (Gibson et al. 1998; Clarke et al. 1987). The generally accepted location of the transition however, is the elongate northeast trending magnetic low region west of Cockburn on the South Australia/New South Wales border (Isles 1983; Mills 1986; Stevens 1986; Ashley et al. 1997). Crooks (2001) challenged the validity of this interpretation, and when looking at the marked conductivity contrast across the Mundi Mundi Fault evident from the current work, it seems more likely that the fault does indeed signify the domain boundary.

CONCLUSIONS

This study has culminated in a number of interesting results and observations. The most striking of these is the marked conductivity contrast across the Mundi Mundi Fault. The conductive Willyama group sediments of the Mundi Mundi Plain and basement rocks from the Olary Domain in the west are one or more orders of magnitude less resistive than the Broken Hill Domain in the east. It is proposed that the rocks of the Broken Hill Domain have minimal fluid content due to earlier granulite facies metamorphism and significant compression during the Delamarian Orogeny. This lack of fluids explains the high (~1000 Ωm) resistivities of these rocks. The compression they experienced

also explains their higher density. The Willyama sediments covering the Olary Domain however are porous and less dense, and therefore have the ability to hold larger quantities of fluids to enhance electrical conductivity.

The location of a highly conducting crustal zone (often referred to as the Flinders Conductivity Anomaly, FCA) was also identified, both from 2D inversions and plots of induction arrows. The FCA has no surface expression, and occurs within the Olary Domain basement, about 50km west of the Broken Hill Domain, and strikes north-south in this area over hundreds of kilometres. Possible mechanisms for the high electrical conductivity of the FCA include crustal fluids and graphite films, although concentrations of copper sulphides have also been located in folded basement structures at Kalkaroo. An interesting hypothesis is that the FCA is linked to the Carpentaria Anomaly that lies east of the Mount Isa Block. The continuity of the conductor may provide a method of linking the Curnamona Province with the Mount Isa Province accurately.

Future work in this region could include the extension of the MT profile to the west, enabling the cross-sectional shape of the FCA to be accurately identified. Also of interest would be a profile perpendicular to the currently accepted boundary between the Olary and Broken Hill Domains, to the south of Cockburn on the South Australia-New South Wales border.

ACKNOWLEDGEMENTS

- Graham Heinson for guidance and support
- Funding from University of Adelaide, PIRSA and ASEG
- Stephan Thiel, Phil Heath, Kate Selway & Dave Baker for field assistance
- MIM for assistance with field work planning
- Wayne Peacock and Antony White (Flinders University) for equipment
- Data sets from Tim Barton, Leijung and Peter Milligan at Geoscience Australia
- WinGLink for Software Support
- Staff and Postgraduate/Honours Students from School of Earth and Environmental Sciences, University of Adelaide

REFERENCES

ASHLEY P.M., COOK N.D.J. & FANNING C.M. 1996. Geochemistry and age of metamorphosed felsic igneous rocks with A-type affinities in the Willyama Supergroup, Olary Block, South Australia, and implications for mineral exploration. *Lithos* **38,** 167-184.

ASHLEY P.M., LAWRIE D.C., CONOR C.H.H. & PLIMER I.R. 1997. Geology of the Olary Domain, Curnamona Province, South Australia and field guide to 1997 excursion stops. *South Australia, Department of Mines and Energy. Report Book 97/17*.

BAILEY R.C. 1990. Trapping of aqueous fluids in the deep crust. *Geophysical Research Letters* **17 (8)**, 1129-1132

BAILEY R.C. 1994. Fluid trapping in mid-crustal reservoirs by H_2O-CO_2 mixtures. *Nature* **371 (6494),** 238-240

CAMPANA B. & KING D. 1958. Regional geology and mineral resources of the Olary Province. *Geological Survey of South Australia, Bulletin* **34,** 133.

CHAMALAUN F.H. 1985. Geomagnetic Depth Sounding experiment in the central Flinders Ranges of South Australia. *Physics of the Earth and Planetary Interiors* **37**, 174-182.

CHAMALAUN F.H. & BARTON C.E. 1990. Comprehensive Mapping of Australia's Geomagnetic Variations. *Eos*, **71**, No 51.

CHAMALAUN F.H. & BARTON C.E. 1993. Electromagnetic induction in the Australian crust: results from the Australia-Wide Array of Geomagnetic Stations. *Exploration Geophysics*, **24** 179-186.

CHAVE A.D. & THOMSON D.J. 1989. Some Comments on Magnetotelluric Response Function Estimation. *Journal of Geophysical Research* **94** No B10 14

CHAVE A.D., THOMSON D.J. & ANDER M.E. 1987. On the robust estimation of power spectra, coherences, and transfer functions. *Journal of Geophysical Research* **92**, 989-1003.

CLARKE G.L., BURG J.P. & WILSON C.J.L. 1986. Stratigraphic and structural constraints of the Proterozoic tectonic history of the Olary Block, South Australia. *Pre-cambrian Research* **34,** 107-137.

CLARKE G.W., GUIRAUD M., BURG J.P.& POWELL R. 1987. Metamorphism of the Olary Block, South Australia: compression with cooling in a Proterozoic fold belt. *Journal of the Metamorphic Geology* **5,** 291-306.

CONOR C.H.H. 2000 Definition of major sedimentary and igneous units of the Olary Domain, Curnamona Province. *MESA Journal* **19,** 51-56.

CONSTABLE S.C. 1985. Resistivity studies over the Flinders Conductivity Anomaly, South Australia. *Geophysical Journal of the Royal Astronomical Society* **83**, 775-786.

COOKE N.D.F. & ASHLEY P.M. 1992. Meta-evaporite sequence, exhalative chemical sediments and associated rocks in the Proterozoic Willyama Supergroup, South Australia: Implications for metallogenesis. *Pre-cambrian Research* **56,** 211-226

CROOKS A.F. 2001. Olary – Broken Hill Domain Boundary. *MESA Journal* **20,** 44-45.

CULL J.P. 1985. Magnetotelluric sounding over a Pre-cambrian contact in Australia. *Geophysical Journal of the Royal Astronomical Society* **80**, 661-675.

DUBA A., HUENGES E., NOVER G., WILL G. & JÖDICKE H. 1988. Impedance of black shale from Münsterland 1 borehole: an anomalous good conductor? *Geophysical Journal* **94**, 413-419

EVERETT, J.E. & HYNDMAN R.D. 1967. Magnetotelluric investigations in south-western Australia. *Physics of the Earth and Planetary Interiors* **1**, 49-54.

FLINT R.B. 1993. Hiltaba Suite in Drexel J.F., Press W.V., and Parker A.J., (eds) The geology of South Australia. Volume 1 The Pre-cambrian. *Geological Survey of South Australia, Bulletin* **54***, 82-93.*

FLINT R.B. & FLINT D.J. 1975. Preliminary geological investigations on the Curnamona 1:250 000 sheet. *South Australia, Department of Mines. Report Book 75/124.*

FLINT R.B. & PARKER A.J. 1993. Willyama Inliers. In Drexel J.F., Preiss W.V., and Parker A.J., (eds) *The Geology of South Australia. Volume 1 the Pre-cambrian. Geological Survey of South Australia*, Bulletin **54**. 82-93.

FROST B.R., FYFE W.S., TAZAKI K. & CHAN T. 1989. Grain-boundary graphite in rocks and implications for high electrical conductivity in the lower crust. *Nature* **340**, 134-136.

GAMBLE T.D., GOUBAU W.M. & CLARKE J. 1979. Magnetotellurics with a remote magnetic reference. *Geophysics* **43**, 53-68.

GIBSON D.L. 1997. Recent tectonics and landscape evolution in the Broken Hill region. *AGSO Research Newsletter* **26**, 17-20

GIBSON G., DRUMMOND B., FOMIN T., OWEN A., MAIDMENT D., GIBSON D., PELIJO M. & WAKE-DYSTER K. 1998. Re-evaluation of Crustal Structure of the

Broken Hill Inlier through Structural Mapping and Seismic Profiling. *AGSO Record, 1998/11.*

GOUGH D.I. 1986 Seismic reflectors, conductivity, water and stress in the continental crust. *Nature* **323,** 143-144

GOUGH, D.I., DE BEER J.H. & VAN ZIIJL J.S.V. 1974. A magnetometer array study in southern Australia. *Geophysical Journal of the Royal Astronomical Society*. **36**, 345-362.

GRAY J.D. & CULL J.P. 1990. Magnetotelluric soundings and resistivity profiles in the Willyama Complex. *Australian Journal of Earth Sciences* **37**, 127-134

GREENHOUSE J.P. & BAILEY R.C. 1981. A review of geomagnetic variation measurements in the eastern United States: implications for continental tectonics. *Canadian Journal of Earth Science*. **18**, 1268-1288.

ISLES D. 1983. A regional geophysical study of the Broken Hill Block, NSW Australia. *University of Adelaide. PhD thesis (unpublished)*

JÖDICKE H. 1985. A large self-potential anomaly at the SE flank of the Stavelot-Venn anticline originating from meta-anthracite bearing black shales at the Salm/Revin boundary. *Neues Jahrb. Geol. Paläcontol. Abb*. **177** 387-402

JONES A.G. 1987. MT and reflection: an essential combination. *Geophysical Journal of the Royal Astronomical Society*. **89** 7-18.

JONES A.G. & FERGUSON I.J. 2001 The electric Moho. *Nature* **409**, 331-333

KATZ M.B. 1976 Lineament tectonics of the Willyama Block and its relationship to the Adelaide aulocogene. *Journal of the Geological Society of Australia.* **23**, 275-285.

KUSZNIR N.J. & PARK R.G., 1986 Continental lithosphere strength: the critical role of lower crustal deformation. *The Nature of the Lower Continental Crust*. 79-93

LAING W.P. 1996. The Diamantina orogen linking the Willyama and Cloncurry Terrains, eastern Australia. In: Pongratz J. and Davidson G.J., (editors) *New developments in Broken Hill Type deposits. Centre for Ore Deposit and Exploration Studies. CODES Special Publications 1. 67-72.*

LILLEY F.E.M. & ARORA B.R. 1982. The Sign Convention for Quadrature Parkinson Arrows in Geomagnetic Induction Studies. *Reviews of Geophysics and Space Physics* **20**, No 3. 513-518.

MARQUIS G. & HYNDMAN R.D. 1992. Geophysical support for aqueous fluids in the deep crust: seismic and electrical relationships. *Geophysical Journal International*. **110**, 91-105

MERZER A.M. & KLEMPERER S.L. 1992 High electrical conductivity in a model lower crust with unconnected, conductive, seismically reflective layers. Geo*physical Journal International.* **108**, 895-905

MILLIGAN P.R., DIREEN N.G. & SHAW R.D. 2000. Geophysical Atlas of the Curnamona Province 1:2 Million Scale. *AGSO*

MILLS A. 1986. An interpretation of regional geophysical data in the Olary region, South Australia. South *Australia, Department of Mines and Energy, Report Book 82/56.*

OLHOEFT G.R. 1981. Electrical properties of granite with implications for the lower crust. *Journal of Geophysical Research*. **86**, 931-936

PARKINSON W.D. 1962. The influence of continents and oceans on geomagnetic variations. *Geophysical Journal of the Royal Astronomical Society*. **4**, 441-449.

PAUL S.K. 1994. Geomagnetic Induction Study of the Adelaide Geosyncline. *Flinders University. PhD Thesis. (Unpublished)*

ROBERTSON R.S., PREISS W.V., CROOKS W.V., HILL P.W. & SHEARD M.J. 1998. Review of the Proterozoic Geology and Mineral Potential of the Curnamona Province in South Australia. *Primary Industries and Resources SA, Report Book 98/3.*

RODI W. & MACKIE R.L. 2001. Nonlinear conjugate gradients algorithm for 2-D magnetotelluric inversion. *Geophysics* **66**, No. 1. 174-187.

RUTLAND R.W.W. 1976. Orogenic Evolution of Australia. *Earth Science Reviews* **12**. 161-196.

SATO H. & IDA Y. 1984 Low frequency electrical impedance of partially molten gabbro: the effect of melt geometry on electrical properties. *Tectonophysics* **107** 105-134

SCHMUCKER U. 1970. Anomalies of geomagnetic variations in the south-western United States. *Bull. Scripps Institute of Oceanography, University of California.* **13**, 165.

SIMPSON F. & WARNER M. 1998. Coincident magnetotelluric, P-wave and S-wave images of the deep continental crust beneath the Weardale granite, NE England: seismic layering, low conductance and implications against the fluid paradigm. *Geophysical Journal International*. **133**, 419-434

STANTON R.L. 1976. Petrochemical studies of the ore environment at Broken Hill, New South Wales: Environmental Synthesis. *Institute of Mining and Metallurgy, Transactions, Section B: Applied Earth Science 85 B221-33.*

STEVENS B.P.J. 1986. Post-depositional history of the Willyama Supergroup in the Broken Hill Block, NSW. *Australian Journal of Earth Sciences* **33**. 73-98

STEVENS B.P.J. 1995. A review of Broken Hill regional geology. In: Mineral Search in the South-West Pacific Region. *8th Edgeworth David Day Symposium, Sydney University 37-50.*

STEVENS B.P.J., BARNES R.G., BROWN R.E., STROUD W.J. & WILLIS I.L. 1988. The Willyama Supergroup in the Broken Hill and Euriowie Blocks, NSW. *Pre-cambrian Research*, **40/41**. 297-327.

STEVENS B.P.J., BARNES R.G. & FORBES B.G. 1990. Willyama Block – regional geology and minor mineralisation. In: Hughes F.E (ed) *Geology of the Mineral Deposits of Australia and Papua New Guinea. Australasian Institute of Mining and Metallurgy. Monograph Series. 14:1065-1072.*

VOZOFF K. 1972. The magnetotelluric method in the exploration of sedimentary basins. *Geophysics*, **37**, 98-141.

THOMSON B.P. 1970. A review of the Pre-cambrian and Lower Proterozoic tectonics of South Australia. *Royal Society of South Australia. Transactions* **94**: 193-221.

THOMSON B.P. 1976. Tectonics and regional geology of the Willyama, Mount Painter and Denison Inlier areas. In: Knight C.L., (ed) *Economic geology of*

Australia and Papua New Guinea. Australasian Institute of Mining and Metallurgy, Monograph 5. 469-76.

THOMSON, D.J. & A.D. CHAVE. 1989. Jacknife error estimates for spectra, coherences, and transfer functions. In: *Advances in Spectral Analysis and Array Processing. Edited by S. Haykin. Prentic Hall, Englewood Cliffs. NJ*

WAFF H. 1974 Theoretical considerations of electrical conductivity in a partially molten mantle with implications for geothermometry. *Journal of Geophysical Research.* **79**, 4003-4010

WANG L.J. & CHAMALAUN F.H. 1995. A magnetotelluric traverse across the Adelaide Geosyncline. *Exploration Geophysics* **26**, 539-546.

WANG L.J., LILLEY F.E.M. & CHAMALAUN F.H., 1997. Large-scale electrical conductivity structure of Australia from magnetometer arrays. *Exploration Geophysics* **28**, 150-155.

WEI W., UNSWORTH M., JONES A., BOOKER J., TAN H., NELSON D., CHEN L., LI S., SOLON K., BEDROSIAN P., JIN S., DENG M., LEDO J., KAY D. & ROBERT B. 2001. Detection of widespread fluids in the Tibetan crust by magnetotelluric studies. *Science* **292**, 716-718.

WILLIS I.L., BROWN R.E., STROUD W.J. & STEVENS B.P.J. 1983. The Early Proterozoic Willyama Supergroup: stratigraphic subdivision and interpretation of high to low-metamorphic rocks in the Broken Hill Block, New South Wales. *Journal of the Geological Society of Australia* **30**. 195-224.

WOODS D.V. & LILLEY F.E.M. 1980. Anomalous geomagnetic variations and the concentration of telluric currents in southwest Queensland, Australia. *Geophysical Journal of the Royal Astronomical Society.* **62**, 675-689.

TABLES

Broken Hill MT Site Locations

Site	Latitude	Longitude	Zone	Easting	Northing	Elevation
B-01	S 031° 41' 41.6"	E 140° 29' 56.3"	54 J	0452519	6493272	120 m
B-02	S 031° 42' 04.0"	E 140° 35' 03.6"	54 J	0460611	6492619	100 m
B-03	S 031° 43' 32.9"	E 140° 39' 45.9"	54 J	0468051	6489907	120 m
B-04	S 031° 44' 24.7"	E 140° 46' 19.4"	54 J	0478408	6488337	119 m
B-05	S 031° 43' 54.1"	E 140° 51' 53.6"	54 J	0487254	6489294	135 m
B-06	S 031° 44' 03.6"	E 140° 37' 48.4"	54 J	0496535	6489010	134 m
B-07	S 031° 44' 20.0"	E 141° 02' 49.6"	54 J	0504462	6488506	150 m
B-08	S 031° 45' 37.9"	E 141° 08' 35.5"	54 J	0513559	6486098	170 m
B-09	S 031° 49' 51.5"	E 141° 11' 42.5"	54 J	0518466	6478284	200 m
B-10	S 031° 53' 45.2"	E 141° 17' 47.3"	54 J	0528034	6471065	276 m
B-11	S 031° 56' 15.7"	E 141° 24' 53.1"	54 J	0539203	6466395	317 m
B-13	S 031° 59' 08.2"	E 141° 31' 39.9"	54 J	0550382	6461034	280 m
B-14	S 032° 02' 31.6"	E 141° 36' 08.4"	54 J	0556868	6454738	240 m
B-15	S 032° 04' 38.1"	E 141° 41' 16.7"	54 J	0564930	6450794	190 m
B-16	S 032° 06' 34.7"	E 141° 46' 42.7"	54 J	0573449	6447148	170 m
K-01	S 031° 48' 35.7"	E 140° 32' 24.3"	54 J	0456468	6480541	120 m
K-02	S 031° 47' 57.4"	E 140° 31' 47.4"	54 J	0455492	6481715	130 m

Table 1 MT Site Locations (As shown in Figure 7)
Latitudes and Longitudes in WGS84, Geographic Coordinates in UTM, Elevations from GPS

FIGURE CAPTIONS

Figure 1 Curnamona Province Geology. After Crooks 2001.

Figure 2 Photograph of topographical transition across Mundi Mundi Fault.

Figure 3 Location of MT and Seismic Lines.

Figure 4 Example of Magnetic time series data.

Figure 5 Example of Electric time series data.

Figure 6 Example of Apparent Resistivity and Phase against period – Station 15.

Figure 7 MT Site locations.
Digital Elevation with Induction arrows and location of Mundi Mundi Fault marked.

Figure 8 MT Equipment Layout

Figure 9 GDS Responses for station 10. The minimal size of most error bars indicate high data quality, with the exception of the higher frequencies in the noise range.

Figure 10 2D Resistivity Modelling. Vertically exaggerated section, RMS = 1.0.
Location of FCA and MMF marked.

Figure 11 AGSO Seismic Line 96AGS-BH1A. After Gibson et al. 1998.

Figure 12 Bouguer Gravity Modelling with 2D Resistivity Inversion section.

Figure 13 Real Parkinson Arrows for 10 and 85 min periods. From Paul (1994)
Inferred Location of FCA marked with dashed line.

Figure 14 Plot of Induction arrows (T~16min) from current study and GA data.
Inferred Location of FCA marked by dashed line.

FIGURES

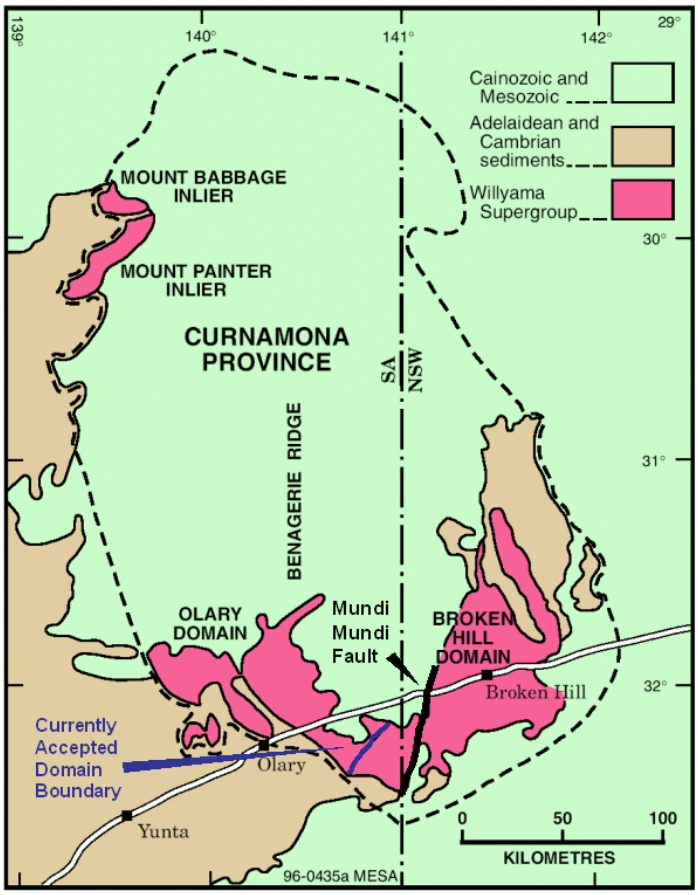

Figure 1 Curnamona Province Geology.
After Crooks 2001.

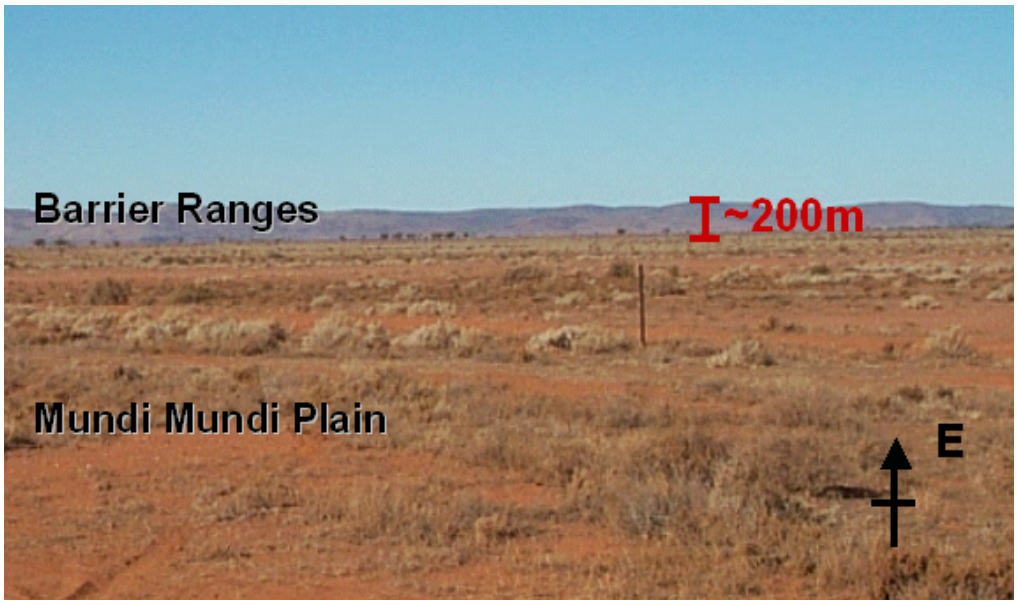

Figure 2 Photograph of topographical transition across Mundi Mundi Fault.

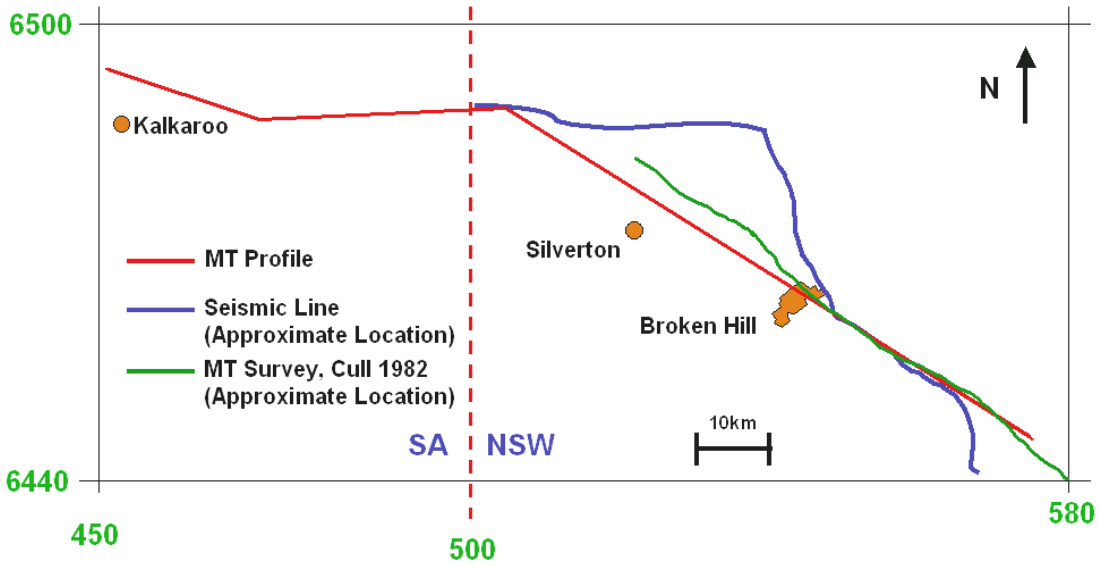

Figure 3 Location of MT and Seismic Lines.

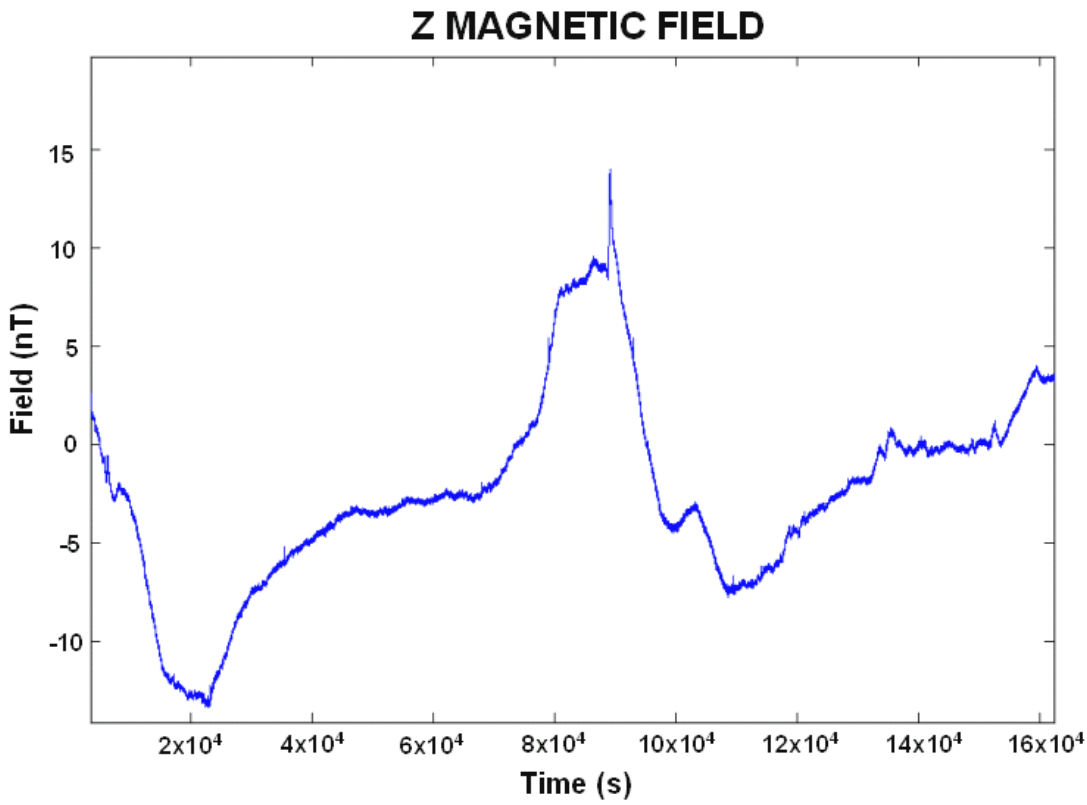

Figure 4 Example of Magnetic time series data.

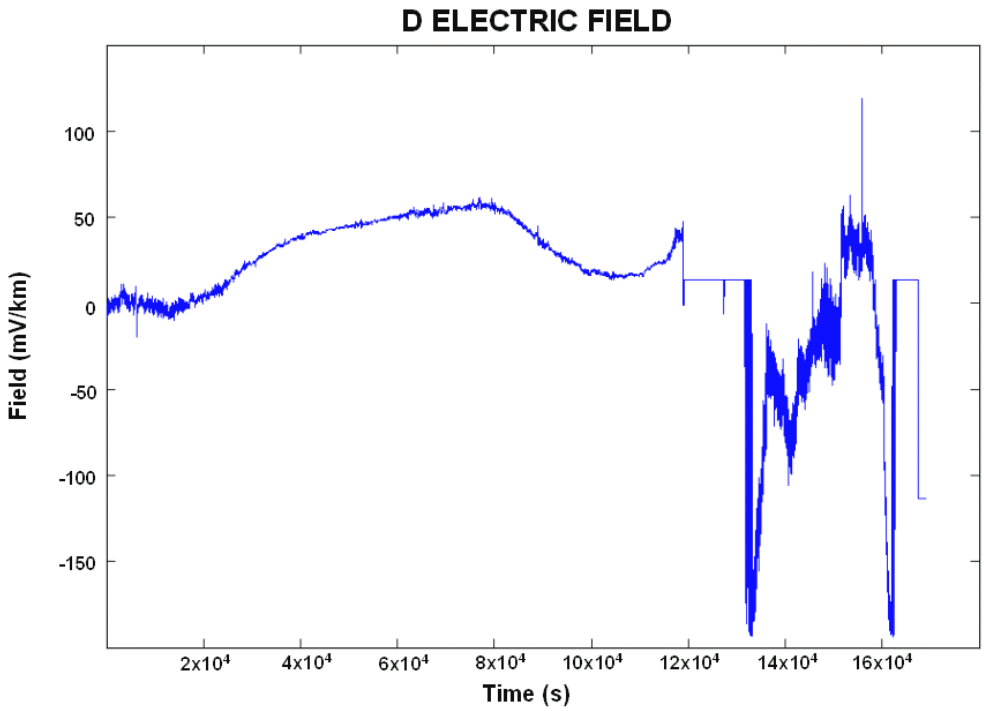

Figure 5 Example of Electric time series data.

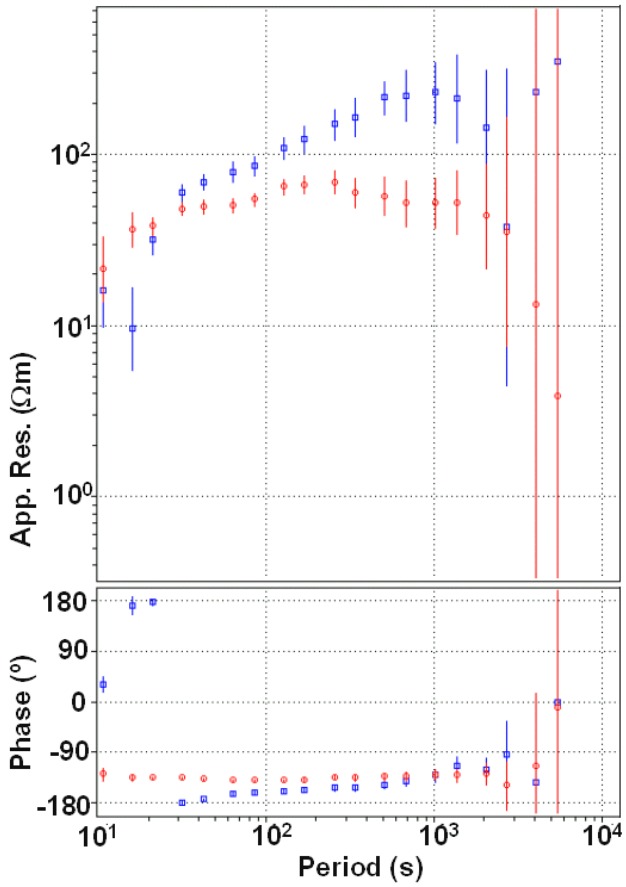

Figure 6 Example of Apparent Resistivity and Phase against period – Station 15.

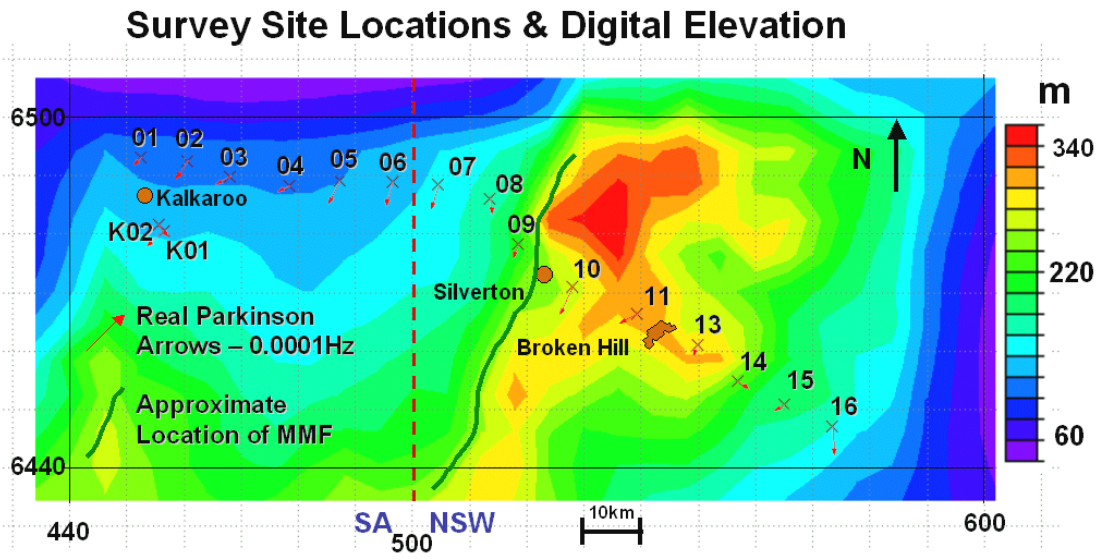

Figure 7 MT Site locations.
Digital Elevation with Induction arrows and location of Mundi Mundi Fault marked.

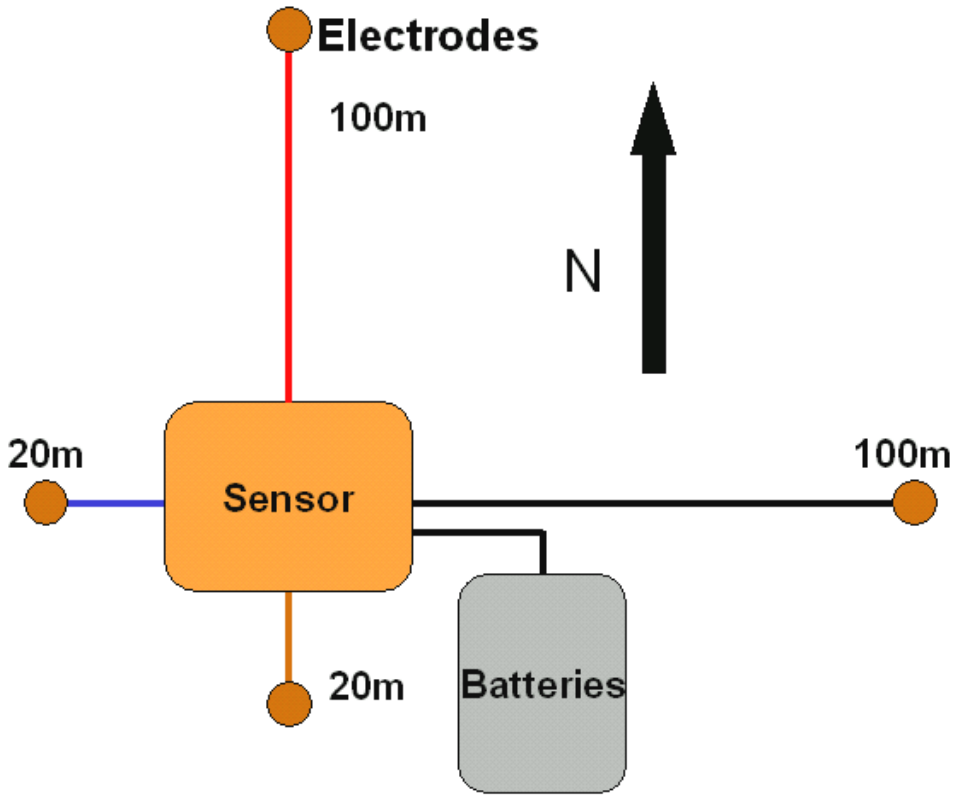

Figure 8 MT Equipment Layout

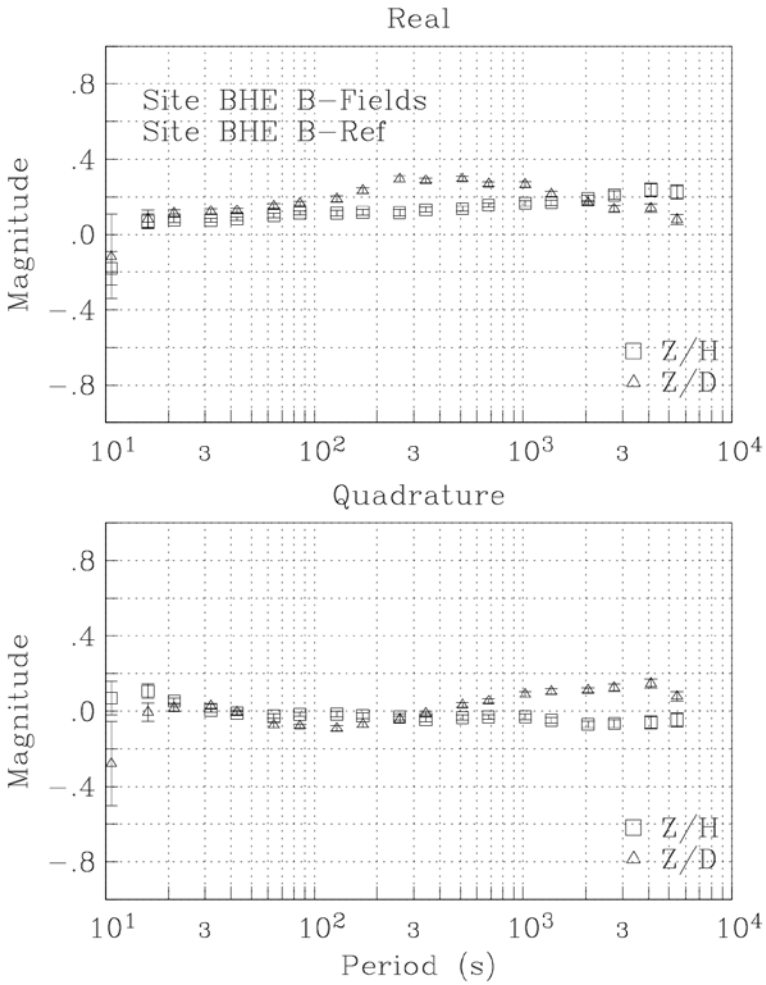

Figure 9 GDS Responses for station 10.
The minimal size of most error bars indicate high data quality, with the exception of the higher frequencies in the noise range.

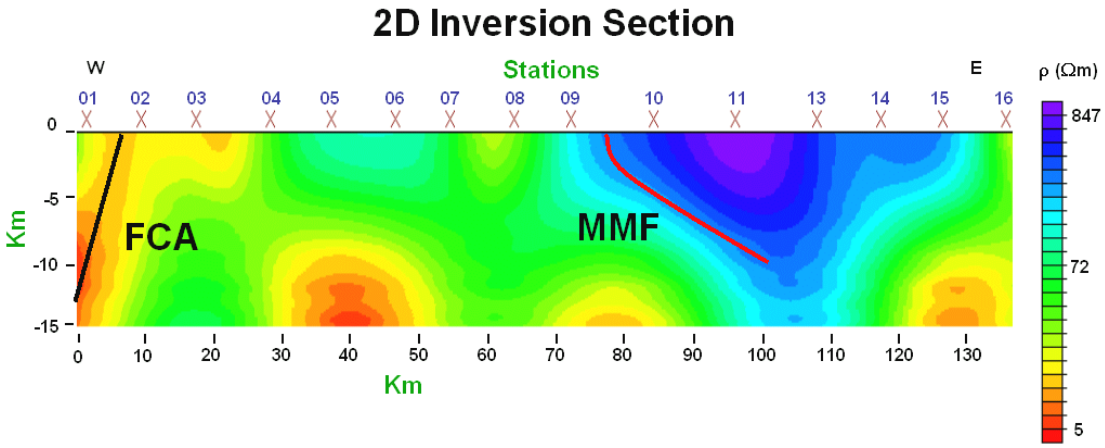

Figure 10 2D Resistivity Modelling.
Vertically exaggerated section, RMS = 1.0. Location of FCA and MMF marked.

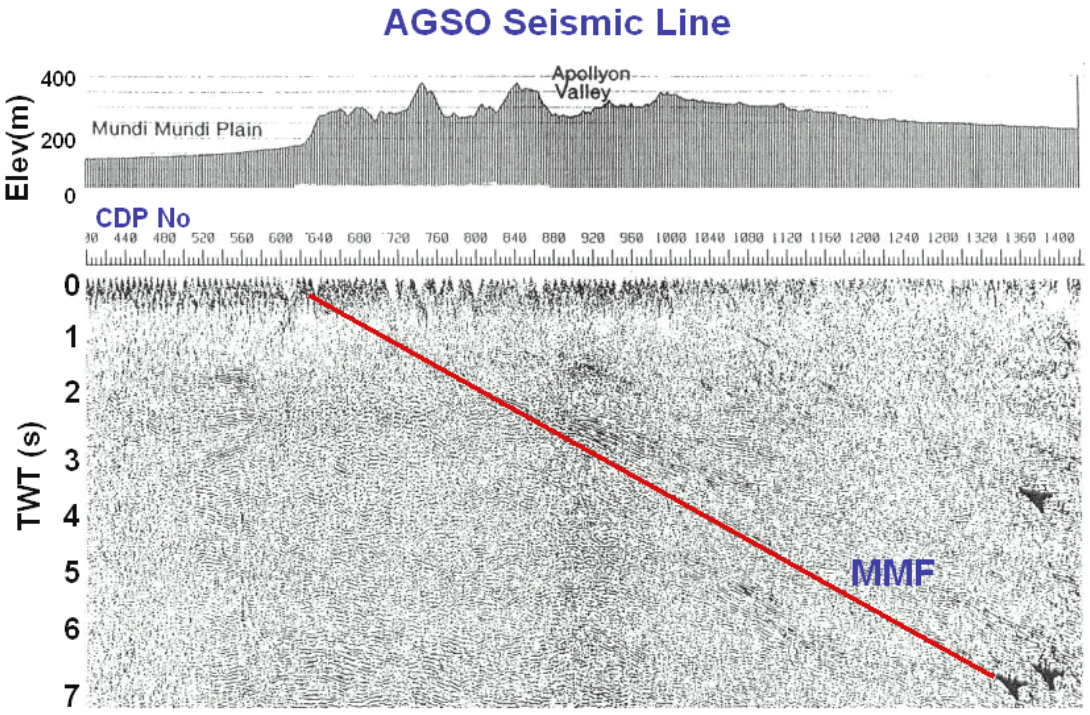

Figure 11 AGSO Seismic Line 96AGS-BH1A.
After Gibson et al. 1998.

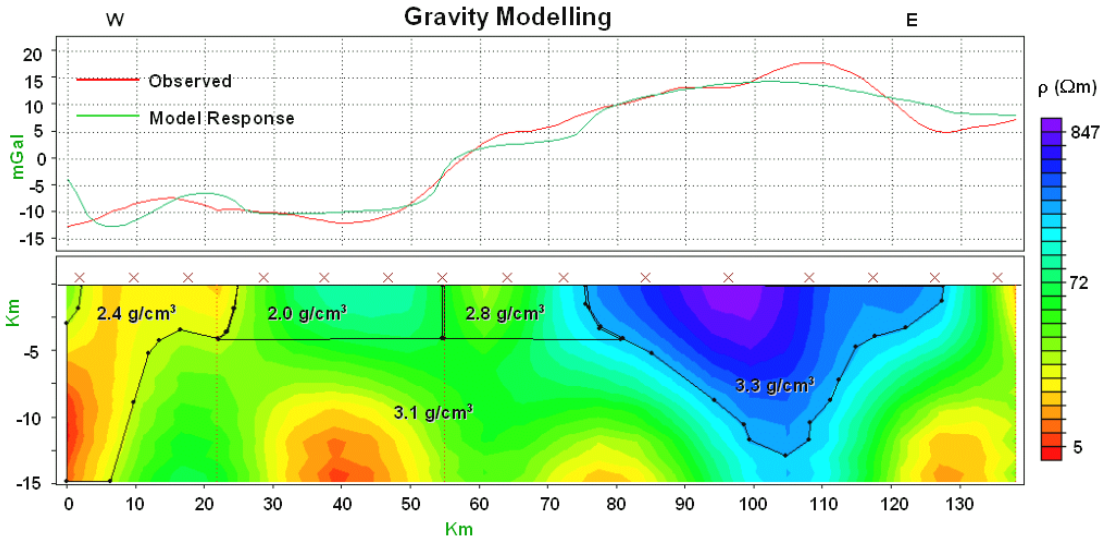

Figure 12 Bouguer Gravity Modelling with 2D Resistivity Inversion section.

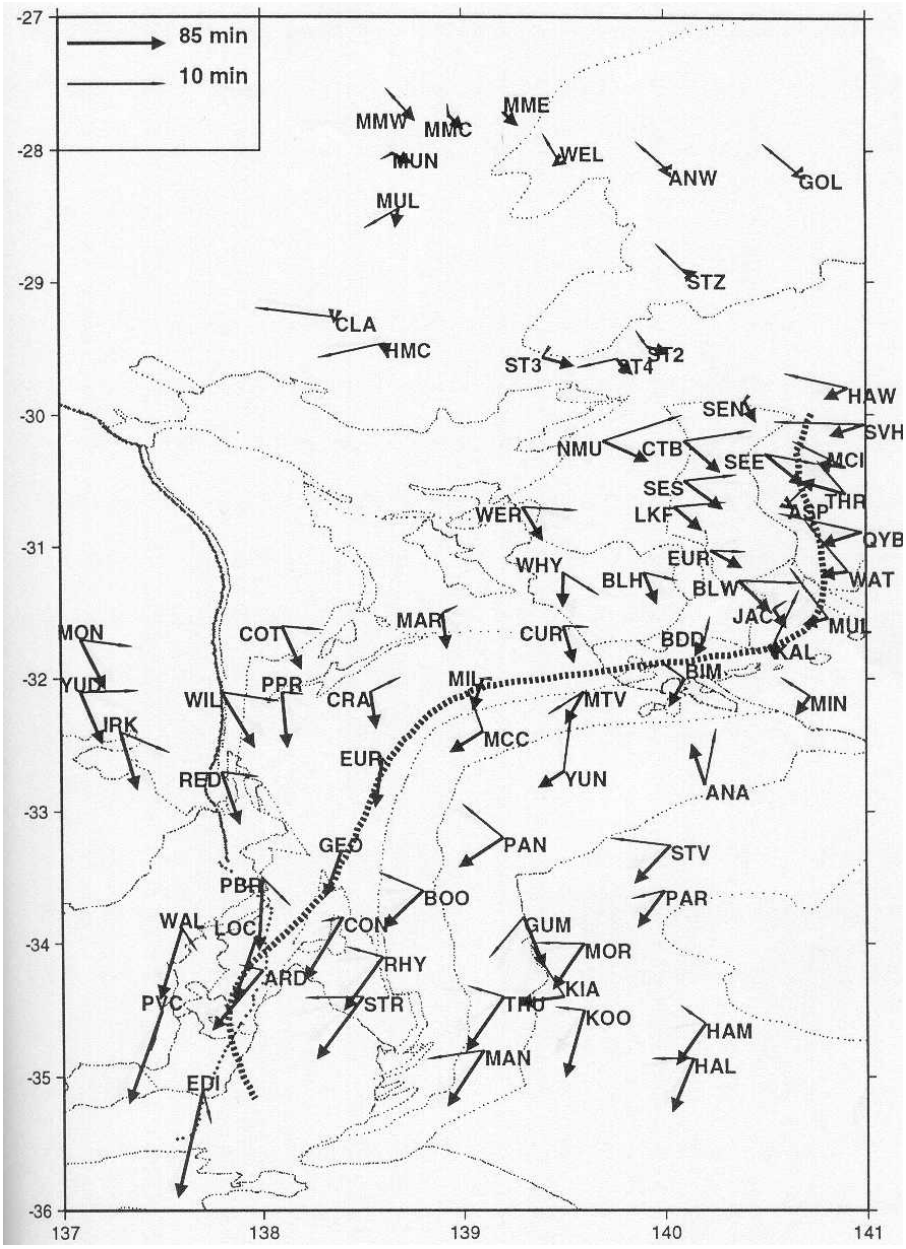

Figure 13 Real Parkinson Arrows for 10 and 85 min periods.
From Paul (1994). Inferred Location of FCA marked with dashed line.

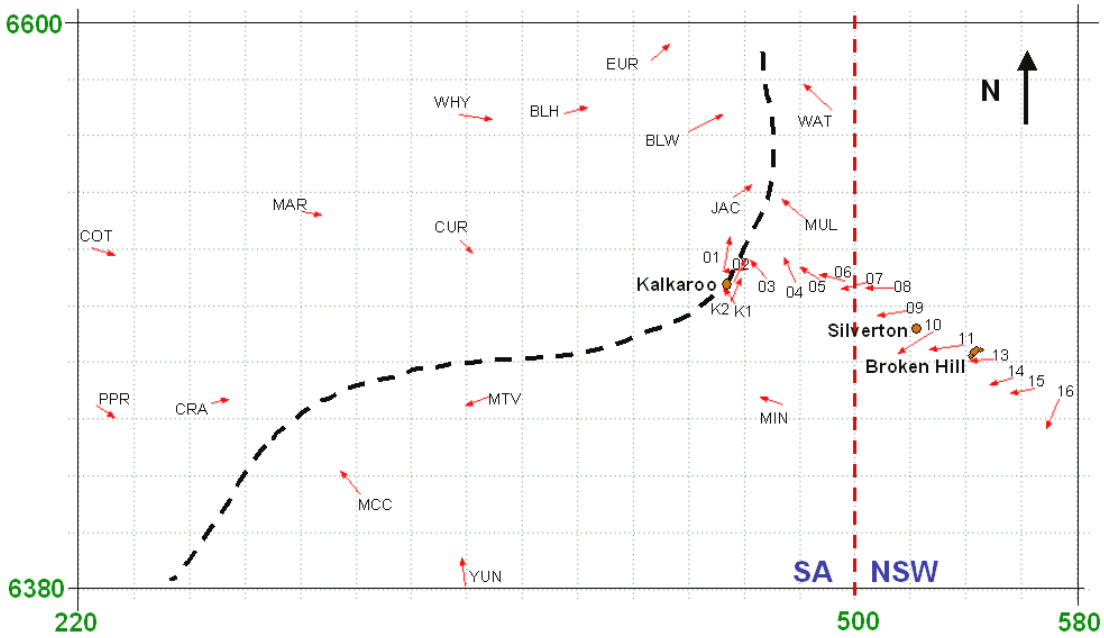

Figure 14 Plot of Induction arrows (T~16min) from current study and GA data. Inferred Location of FCA marked by dashed line.